Biological and Pharmaceutical Bulletin Advance Publication by J-STAGE
DOI:10.1248/bpb.b20-00994

Advance Publication
December 23, 2020

PTP1B Inhibitory and Anti-inflammatory Properties of Constituents from *Eclipta prostrata* L.

Duc Dat Le,[a,b,c] Duc Hung Nguyen,[a,d] Eun Sook Ma,[a] Jeong Hyung Lee,[e]

Byung Sun Min,[a] Jae Sue Choi,[f] and Mi Hee Woo[a,*]

[a]College of Pharmacy, Drug Research and Development Center, Daegu Catholic University, Gyeongsan 38430, Republic of Korea

[b]Division of Computational Physics, Institute for Computational Science, Ton Duc Thang University, Ho Chi Minh City, Vietnam.

[c]Faculty of Pharmacy, Ton Duc Thang University, Ho Chi Minh City, Vietnam.

[d]Department of Biotechnology, V-Kist, Hanoi Vietnam.

[e]College of Natural Science, Kangwon National University, Kangwon 200-701, Republic of Korea

[f]Department of Food and Life Science, Pukyong National University, Busan 48513, Republic of Korea

*Corresponding author.
E-mail addresses: woomh@cu.ac.kr (M.H. Woo).
Daegu Catholic University, Gyeongsan 38430, Republic of Korea

The white-flowered leaves of *Eclipta prostrata* L. together with leaves of *Scoparia dulcis* and *Cynodon dactylon* are mixedly boiled in water and given to diabetic patients resulting in the significant improvement in the management of diabetes. However, the active constituents from this plant for antidiabetic and anti-obesity properties are remaining unclear. Thus, this study was to discover anti-diabetes and anti-obesity activities through PTP1B inhibitory effects. We found that the fatty acids (**23** and **24**) showed potent PTP1B inhibition with IC_{50} values of 2.14 and 3.21 μM, respectively. Triterpenoid-glycosides (**12**–**15**) also exhibited strong to moderate PTP1B inhibitory effects, with IC_{50} values ranging from 10.88 to 53.35 μM. Additionally, active compounds were investigated for their PTP1B inhibitory mechanism and docking analysis. On the other hand, the anti-inflammatory activity from our study revealed that compounds (**1**–**4**, **7**, **8**, and **10**) displayed the significant inhibition NO production in LPS-stimulated RAW264.7 cells. Especially, compound **9** showed the potent inhibitory effects in lipopolysaccharide (LPS)-induced NO production on RAW264.7 cell. Therefore, further Western blot analysis was performed to identify the inhibitory expression including heme oxygenase-1 (HO-1) and IκB phosphorylation.

Keywords *Eclipta prostrata* L.; PTP1B; molecular docking analysis; NO inhibition; inflammation.

INTRODUCTION

Insulin-mediated signal transduction occurs in the balance between tyrosine phosphorylation and de-phosphorylation at the earliest steps, namely insulin receptor (IR) and its primary substrates (insulin receptor substrate proteins, IRS). Protein tyrosine phosphatases (PTPs) are negative regulators in normal physiological states that play an important role in transduction of insulin resistance.[1)] Among PTPs family member, PTP1B is known to be a key negative regulator of insulin and leptin signaling pathway. Deficiency of PTP1B could remain sustained phosphorylation process of insulin receptor, leading to insulin sensitivity and improved glucose tolerance[2)] as well as resistance to weight gain through their leptin sensitivity improvement.[3)] Thus, PTP1B inhibitor may be useful for treating diabetes mellitus and obesity diseases.

Eclipta prostrata L. belongs to *Eclipta* genus of family of Asteraceae (Compositae). This plant is used as traditional medicine for treatment of infectious hepatitis, jaundice, liver cirrhosis, aching and weakness of the knees and loins, spitting of blood, epistaxis, hematuria and diarrhea with bloody stools, abnormal uterine bleeding, hepatic diseases, and hyperlipidemia.[4,5)] *E. prostrata* has attracted a great deal of attention due to its wide range of biological effects including antitumor,[6)] anti-inflammatory,[7)] antimicrobial, antioxidant, immunomodulatory, hepatoprotective, analgesic, and hair growth promoting activities.[8)] Notably, white-flowered leaves from this plant are mixed with leaves of *Scoparia dulcis* and *Cynodon dactylon* in water, and then boiled in an earthen vessel. The water is then strained through cloth and given to diabetic patients to be taken orally in the morning and evening on an empty stomach in Thakurgaon district of Bangladesh. In India, this plant is known in the three major forms of Indian traditional medicinal systems, namely, Ayurveda, Unani, and Siddha, respectively. Among Ayurvedic system products, Trasina contains the ingredients of *E. prostrata*. This

functional product is one of the largest selling Ayurvedic antihyperglycemic drug (Dey's Medical, Calcutta) in India. In view of above information, a study from *E. prostrata* leaves showed a significant reduction of blood glucose level.[9] Crude extract of *E. prostrata* also exhibits antihyperlipidemic property by reducing elevated lipid, cholesterol, triglycerides, phospholipids, and free fatty acids levels.[10] However, the active constituents from *E. prostrata* for antihyperglycemic and antihyperlipidemic effects have not been identified until now.

Diabetes mellitus may be associated with oxidative and inflammation stress by increasing their levels in patients. Inflammation associated to innate and adaptive immune systems is a normal response to infection. However, inflammation for long term may result in autoimmune or auto-inflammatory disorders, neurodegenerative disease, or cancer.[11] Thus, it is necessary to control inflammation process effectively.

The present study was to find out constituents from *E. prostrata* for anti-diabetes and anti-obesity properties based on their PTP1B activity. Furthermore, the anti-inflammatory effects of the isolates were also investigated through NO inhibitory activities in LPS-stimulated RAW 264.7 cells.

MATERIALS AND METHODS

General Experimental Procedures The optical rotations were performed on a JASCO DIP–370 digital polarimeter (Jasco, Easton, MD, USA). The IR spectra were obtained from JASCO FT/IR–4100 spectrometer (Jasco, Easton, MD, USA). UV spectra were operated in MeOH by using a Shimadzu spectrophotometer (Chiyoda, Tokyo, Japan). The nuclear magnetic resonance (NMR) spectra were recorded on an Oxford AS 400 MHz instrument (Varian, Palo Alto, CA, USA), and the chemical shifts were reported as δ values with TMS as the internal standard [measured in methanol-d_4, pyridine-d_5, chloroform-d_1 (Merck, Darmstadt, Germany)].

The (ESI-MS) spectra were obtained using an Agilent 6530 Accurate–Mass Q–TOF LC/MS system. Open column chromatography (CC) experimented on silica gel (Merck, Darmstadt, Germany; 63−200 μm particle size), YMC RP–18 (Merck, Darmstadt, Germany; 150 μm particle size). Thin layer chromatography (TLC) used pre–coated silica gel 60 F_{254} (1.05554.0001, Merck, Darmstadt, Germany) and RP–18 F_{254S} plates (1.15685.0001, Merck, Darmstadt, Germany) and were visualized by spraying with aqueous 10% H_2SO_4 and heating for 3–5 min.

Plant Material The aerial parts of *E. prostrata* were collected from Yeongcheon, Gyeongsangbuk-do, Republic of Korea in August 2016. The plant species was identified by Professor Byung Sun Min, College of Pharmacy, Catholic University of Daegu, Republic of Korea. A voucher specimen (DCU-201608) was deposited at the Herbarium of the College of Pharmacy, Catholic University of Daegu, Republic of Korea.

Extraction and isolation The dried leaves of *E. prostrata* (15 kg) were extracted with ethanol (4L x 4 times in 48 hours) at room temperature. The solution was evaporated under reduced pressure to give residue (1.1 kg). This residue was suspended in water and partitioned successively with each volume of 5 L x 3 times of *n*-hexane, CH_2Cl_2, EtOAc, and *n*-BuOH, yeilding *n*-hexane fraction (285 g), CH_2Cl_2 fraction (315 g), EtOAc fraction (100 g), and *n*-BuOH fraction (290 g), respectively. The EtOAc fraction (100 g) was fractionated by open column chromatography [silica gel, 20–100% (v/v)] with the methylene chloride–methanol gradient solvent system, collecting 10 fractions (EPE1–EPE10). These parts were combined and evaporated by analyzed their TLC profiles using EtOH (10% H_2SO_4) solution on heating. The EPE4 (3.5 g) was subjected on reverse phase (YMC RP-18) open column chromatography eluting with acetone–water (1/1.8, v/v) solvent system to obtain compounds **18** (8.5 mg), **19** (6.5 mg), and further purified on silica gel using solvent system of methylene chloride–methanol

(10/1, v/v) to get compounds **1** (15 mg), **17** (5.9 mg) and **20** (7.2 mg), respectively. Sub-fraction EPE7 (1.5 g) was chromatographed on Sephadex LH-20 eluting with methanol–water (1/1, v/v) solvent system to get compounds **5** (8.5 mg) and **11** (20 mg), and further purified on reverse phase (YMC RP-18) open column chromatography acetone–water (1/2.5, v/v) solvent system to yield compounds **12** (10.2 mg) and **22** (9.5 mg). *n*-BuOH fraction (125 g) was loaded to open column chromatography [silica gel, 35–100% (v/v)] with the methylene chloride–methanol gradient solvent system, collecting 12 fractions (EPB1– EPB12). Sub-fraction EPB1 (1.3 g) was separated on reverse phase (YMC RP-18) open column chromatography eluting with acetone–water (from 1/2.5 to 1/1, v/v) gradient solvent system to obtain **9** (8.2 mg) and **16** (10.5 mg). Sub-fraction EPB2 (2.5 g) was chromatographed on Sephadex LH-20 eluting with methanol–water (1/1, v/v) solvent system to get compounds **4** (7.6 mg), **21** (9.1 mg), and further purified on reverse phase (YMC RP-18) open column chromatography eluting with acetone–water (from 1/1.5, v/v) solvent system to obtain **2** (6.9 mg) and **13** (11 mg). Fraction EPB3 (3.5g) was loaded on reverse phase (YMC RP-18) open column chromatography eluting with acetone–water (from 1/1.5, v/v) solvent system to afford compound **3** (11 mg), and further purified on open column chromatography silica gel with the methylene chloride–methanol (10/1.5, v/v) solvent system, collecting **6** (10.2 mg) and **8** (7.1 mg). Fraction EPB5 (2.6 g) was loaded on reverse phase (YMC RP-18) open column chromatography eluting with methanol–water (1/1.2, v/v) solvent system to afford compounds **7** (9.1 mg), **14** (7.9 mg), and further purified on Sephadex LH-20 eluting with methanol (100 %) to get compounds **10** (8.6 mg) and **15** (6.9 mg). Fraction EPB6 (0.5 g) was subjected on reverse phase (YMC RP-18) open column chromatography eluting with acetone–water (1.5/1, v/v) solvent system to afford compounds **23** (12.0 mg) and **24** (8.2 mg), separately.

PPT1B assay PTP1B (human, recombinant) was purchased from Biomol International LP (USA) and the enzyme activity was operated using *p*-nitrophenyl phosphate (*p*-NPP) as a substrate.[12] In particularly, the PTP1B hydrolysis process from *p*-NPP to *p*-nitrophenol (*p*-NP) production could be detected at 405 nm. In each 96-well plates (total 200 μL of volume), there were 2 mM *p*-NPP and PTP1B (0.05–0.1 μg) in a buffer containing 50 mM citrate (pH 6.0), 0.1 M NaCl, 1 mM EDTA, and 1 mM dithiothreitol (DTT) with or without test compound, following by pre-incubated at 37°C for 10 min, and then implemented with 50 μL of *p*-NPP. The reaction was finally added with 10 M NaOH. The amount of product (*p*-NP) was measured the absorbance at 405 nm. The excess amounts of 2 mM *p*-NPP were determined with absorbance at 405 nm obtained in the absence of PTP1B enzyme. The PTP1B inhibitory activity of each sample was determined by the equation:

Inhibition (%) = [1 − (sample OD − blank 2 OD) / (control OD − blank 1 OD)] × 100

whereas OD is absorbance at 405 nm. Ursolic acid was used as positive control.

PTP1B enzyme kinetic assay The enzymatic assay was performed as the same PTP1B assay method. The assay consisted of different *p*-NPP concentrations as a PTP1B substrate in the presence at various concentrations of test compounds. The inhibitory mechanism was determined through the Dixon plot for various substrate concentrations and the Lineweaver-Burk plot for various test compound concentrations.[13] The inhibition constants (K_i) of enzyme-inhibitors complex were obtained from the interpretation of Dixon plots.

Cell culture and MTT assay for cell viability The RAW264.7 cells were maintained in Dulbecco's Modified Essential. These cells were grown at 37 ^{o}C in DMEM supplemented with 10% heat-inactivated FBS, penicillin (100 units/mL), and streptomycin sulfate (100 μg/mL) in a humidified atmosphere of 5% CO_2. After pre-incubation of RAW264.7 cells for 4 h, 0–10

μg/mL each compound was added. RAW264.7 viability after 24 h of continuous exposure to the compounds was measured with a colorimetric assay based on the ability of mitochondria in viable cells to reduce MTT. Briefly, 1×10^4 cells/well treated for 24 h with vehicle or compounds were examined for cell viability. Viability of the macrophages treated with vehicle (0.5% DMSO) only was defined as 100% viable. Survival of macrophage cells after treatment with compounds was calculated using the following formula: viable cell number (%) = OD_{570} (treated cell culture)/OD_{570} (vehicle control) × 100.

Determination of NO production and the cell viability assay The level of NO production was determined by measuring the amount of nitrite from the cell culture supernatants as described previously.[14] Briefly, the RAW264.7 cells (1×10^5 cells/well) were stimulated with or without 1 μg/mL of LPS (Sigma Chemical Co., St. Louis, MO) for 24 h in the presence or absence of the test compounds (3–50 μM). The cell culture supernatant (100 μL) was then reacted with 100 μL of Griess reagent. The remaining cells after the Griess assay were used to test their viability using MTT (Sigma Chemical Co., St. Louis, MO)-based colorimetric assay. Cell viability was determined by the mitochondria-dependent reduction of MTT [3-(4,5-dimethyl-thiazol-2-yl)-2,5-diphenyltetrazolium bromide] to formazan. Cell in 96-well plates were incubated at 37 °C with MTT (5 mg/mL for 4 h). Cultured medium was gently aspirated from each well, and then the MTT crystals were dissolved in acid-SDS (100 μg). The reduction of the MTT to formazan within the cells was quantitated by measurement of the OD_{570} against OD_{630}.

Immunoblot analysis Proteins were extracted from cells in ice-cold lysis buffer (50 mM Tris–HCl, pH 7.5, 1% Nonidet P-40, 1 mM EDTA, 1 mM phenylmethyl sulfonyl fluoride, 1

μg/mL leupeptin, 1 mM sodium vanadate, 150 mM NaCl). Fifty microgram of protein per lane was separated by sodium dodecyl sulfate (SDS)–polyacrylamide gel electrophoresis (PAGE) and followed by transferring to a polyvinylidene difluoride membrane (Millipore, Bedford, MA, USA). The membrane was blocked with 5% skim milk, and then incubated with the corresponding antibody. Antibodies for COX-2 and iNOS were obtained from Santa Cruz Biotechnology (Santa Cruz, CA, USA). Antibody for α-tubulin was purchased from Sigma. After binding of an appropriate secondary antibody coupled to horseradish peroxidase, proteins were visualized by enhanced chemiluminescence according to the instructions of the manufacturer (Amersham Pharmacia Biotec, Buckinghamshire, UK).

Statistical analysis Data was represented as the means ± standard deviations of three replicates. The student *t*-test was used for statistical analyses of the difference noted. $P < 0.01$ was accepted as statistically significant.

Molecular docking analysis The prediction of protein (PTP1B)-ligand interactions is important for the success of the virtual-screening approaches. The Autodock vina 1.1.2 program was used to estimate the conformation of the protein-isolated compound complex. The 3D structure of the protein target (NCBI protein ID: 1NNY for human AR) was used for the docking studies without further modification. The ligand 3-({5-[(*N*-acetyl-3-{4-[(carboxy)-(2-carboxyphenyl)amino]-1-naphthyl}-*L*-alanyl)amino]pentyl}oxy)-2-naphthoic acid (3-NNA) was identified in the formed crystal structure. Then, the control ligand was docked back to the corresponding binding pocket to reproduce the orientation and position of the inhibitor observed in the crystal structure. Subsequently, the active compounds were docked using the optimal orientation of the docked domains for 3-NNA. The binding sites were determined by Discovery

Studio software (ver. 4.1). Finally, the inhibitory effects of potential active isolates on protein were evaluated by molecular docking model.

RESULTS

Isolation and identification of isolated compounds from the Aerial Parts of *E. prostrata* Firstly, we found that ethanolic crude extract of *E. prostrata* displayed potent PTP1B inhibitory effect (PTP1B inhibition rate of 65% at concentration of 100 μg/mL). The bioassay–guided isolation led to 24 compounds (**1**–**24**) from ethanolic extract of *E. prostrata*. Structures of all isolates have been elucidated by spectroscopic and spectrometric analyses, including luteolin (**1**),[15] (luteolin-7-*O*-*β*-D-glucoside (**2**),[15] quercetin-3-*O*-*β*-D-glucoside (**3**),[16] apigenin (**4**),[17] tricetin (**5**),[18] kaemferol-7-*O*-*α*-D-rhamnoside (**6**),[19] hesperetin-7-*O*-*β*-D glucoside (**7**),[20] orobol (**8**),[17] 7-*O*-methylorobol-4′-*O*-*β*-D-glucopyranoside (**9**),[21] orobol 7-*O*-*β*-D-glucoside (**10**),[22] wedelolactone (**11**),[6] eclalbasaponin I (**12**),[6] eclalbasaponin II (**13**), eclalbasaponin III (**14**), eclalbasaponin V (**15**),[23] machaeroceric acid (**16**),[24] stigmasterol glucoside (**17**),[25] syringic acid (**18**), procatechuic acid (**19**),[26] vanilic acid (**20**),[27] 4-hydroxybenzoic acid (**21**),[28] chlorogenic acid (**22**),[29] (2*S*)-1-*O*-stearoyl-3-*O*-*β*-D-galactopyranosyl-*sn*-glycerol (**23**),[30] and (2*S*)-3-*O*-(9*Z*,12*Z*-octadecadienoyl)glyceryl-*O*-*β*-D-galactopyranoside (**24**).[31] (Figure 1).

PTP1B inhibitory activity of isolates (1–24) from *E. prostrata* Hyperglycemia is the most common characteristic of type 2 diabetes mellitus, while targeting hyperglycemia with PTP1B inhibitors has proven to be beneficial to glycemic control and thus to the treatment of type 2 diabetes.[32]

Continuation of our research to find PTP1B inhibitors from nature,[12] all isolates (**1**–**24**) were tested for their inhibitory effects on PTP1B enzyme. Results revealed that two fatty acids **23** and **24** showed the most potent inhibitory effects, with IC_{50} values of 2.14 ± 0.09 and 3.21 ±

0.13 μM, respectively, stronger than ursolic acid, a positive control (IC_{50}: 12.00 ± 0.71 μM). This result notably indicates important physiological function of fatty acid. Fatty acid may upregulate lipid metabolism of diabetes and insulin sensitivity, decrease the incidence of obesity, facilitate weight loss, and help maintenance of body weight.[32] Additionally, saponin compounds (**12**–**15**) exhibited significant inhibition on PTP1B enzyme. Among saponins, compounds **13**, **14**, and **15** displayed strong inhibition, with IC_{50} values of 11.75 ± 0.20, 15.23 ± 0.85, and 10.88 ± 0.97 μM, respectively. Compound **12** showed moderate inhibitory activity, with IC_{50} value of 53.35 ± 3.96 μM. However, compound **16** was inactive (IC_{50} >100 μM). Among flavone and isoflavone, compound **7** showed the strongest inhibitory activity (IC_{50} 14.11 ± 1.17 μM) while compounds **1**, **2**, **4**, and **9** displayed significant inhibition, with IC_{50} values of 82.40 ± 3.08, 81.77 ± 1.87, 45.50 ± 2.60, and 53.94 ± 1.45 μM, respectively. Other ones in these flavone group showed inactive activity (IC_{50} >100 μM). Phenolic compounds **21** and **22** showed moderate inhibition, with IC_{50} values of 48.70 ± 5.50 and 59.87 ± 5.48 μM, respectively. In contrast, other phenolics and sterol showed inactive PTP1B inhibition (IC_{50} >100 μM) (Table 1).

Compounds **12**–**16** belong to oleanane triterpene group. Compound **16** without sugar moiety did not show PTP1B inhibitory effect. Thus, saponins having glucopyranosyl moiety are favorable for inhibiting PTP1B enzyme at tested condition. Compound **9** containing methoxyl group at C-7 showed the strongest inhibitory effect in isoflavone series (**8**–**10**). Similarity, compound **7** having a methoxyl group showed the strongest PTP1B inhibitory activity among flavones (**1**–**7**).

Enzyme kinetic analysis of active compounds against PTP1B Strongly active compounds **7**, **13**–**15**, **23**, and **24** were further subjected to enzyme kinetic assay to clarify their potent activity against PTP1B. According to Lineweaver-Burk plot and secondary plot of *y*-intercept

(Table 1 and Figure S, supporting materials), compounds **7**, **13**, **14,** and **24** showed mixed type inhibition against PTP1B whereas compounds **15** and **23** showed inhibition in a competitive manner. Binding constant of inhibitor with enzyme-substrate complex (K_{iu}) and free enzyme (K_{ic}) was determined using the secondary plot of $1/V_{max,app}$ (*Y-intercept*) and $K_{m,app}$ / $V_{max,app}$ (*slope*) of the respective linear regression of Lineweaver-Burk plot. As shown in Figure S2 (Supporting materials), K_i values of **7**, **13**, **14**, and **24** for inhibiting PTP1B were 9.3, 9.97, 15.79, and 3.39 μM, respectively. K_i values for inhibiting PTP1B by **15** and **23** were 11.65 and 2.01 μM, respectively.

Molecular docking simulation in PTP1B inhibition The PTP1B inhibitors was simulated base on their structures apply for developing novel therapeutic drugs with selectivity and cell permeability. The structural features of PTP1B consisted of 435 amino acids, containing residues 30–278, which implicate the catalytic domain. Compounds **7**, **13**–**15**, **23**, and **24** exhibited strong inhibition on PTP1B. Thus, these compounds were evaluated for their binding affinities and aspects using computational docking analysis. The docking simulation was performed along with amino acid residues involved to H-bonds, hydrophobic, and electrostatic interactions. Considering docking results of tested inhibitors (**7**, **13**–**15**, **23**, and **24**) together with 3-(3,5-dibromo-4-hydroxy-benzoyl)-2-ethyl-benzofuran-6-sulfonic acid (4-sulfamoyl-phenyl)-amide (an allosteric inhibitor) and 3-({5-[(*N*-acetyl-3-{4-[(carboxycarbonyl)(2-carboxyphenyl)amino]-1-naphthyl}-L-alanyl)amino]pentyl}oxy)-2-naphthoic acid (compound **23**, an catalytic inhibitor), compounds **7**, **13**, **14,** and **24** were stably posed in similar catalytic domains of PTP1B residues containing Cys215, Arg221, Tyr20, and Asp48 (Figure S3). In addition, the binding energies of these compounds (–8.1, –8.4, –8.1, and –6.0 kcal/mol, respectively) (Table S1) indicated the high affinity to PTP1B residues comparing to that of standard catalytic inhibitor (–19.2 kcal/mol).

Whereas, these compounds also posed in allosteric domains of PTP1B residues including Asn193, and Glu276 (Figure S4) with binding energy of –8.2, –7.7, –7.5, and –6.3 kcal/mol comparing to those of allosteric inhibitor of –13.3 kcal/mol, respectively (Table S1).

Effect of the isolated compounds (1–24) on the viability of RAW 264.7 macrophage cells To obtain a suitable concentration range for investigating the effects of the isolated compounds (**1**–**24**) on RAW 264.7 cell viability, cells were treated with concentrations ranging from 3 to 50 μM and later treated with LPS (1 μg/mL) for 24 h using MTT assay.[14)] There were no significant alterations in cell viability following EP extract treatment at these concentrations (data not shown).

Inhibitory effects of isolated compounds (1–24) on LPS-Induced Production of NO in RAW 264.7 Cells RAW 264.7 cells were treated with 3, 10 and 50 μM of the isolates, with and without stimulation with LPS, to determine whether the compounds inhibited NO production. The LPS increased NO production, compared to that in untreated cells. The active compounds (**1**–**4**, **7**–**10**, and **20**) inhibited these increases at a dose dependence of different concentrations. The NO levels were quantified using the Griess reaction. Notably, compounds **1**–**4**, **7**, **8**, and **10** showed the strong NO inhibitory effects in LPS-stimulated RAW 264.7 cells with IC_{50} values ranging from 12.16 – 17.98 μM, respectively. Compound **20** showed the moderate inhibition with IC_{50} value of 40.81 ± 0.14 μM. Especially, compound **9** exhibited the potent inhibition on NO production with IC_{50} less than 1 μM. Other compounds displayed the weak or inactive inhibitory effects (IC_{50} values > 50 μM) (Table 1).

Effect of the compound 9 on LPS-Induced IκB Phosphorylation in RAW 264.7 Cells Compound **9** showed the potent inhibition at concentration less than 1 μM. Thus, this compound was further assayed at the lower inhibitory concentration of 0.1, 0.3 and 1 μM at the same

experiment condition which was above described. As shown in Figure 2, compound **9** extremely inhibited NO production in LPS-stimulated on RAW264.7 cells with IC_{50} value of 0.27 ± 0.01 μM.

To investigate the anti-inflammatory mechanism of compound **9**, further experiment was designed to confirm whether compound **9** activates Nrf2 in RAW264.7 cells. The result indicated that treatment of compound **9** on RAW264.7 cells did not increase HO-1 level in a time-dependent manner (Fig. 2). Compound **9** showed the negative effect on HO-1 expression level by Western blot analysis. Thus, we examined whether compound **9** suppressed LPS-induced activation of NF-κB, which is a well-known and important transcription factor that regulates pro-inflammatory mediator synthesis, such as iNOS, IL-6, and TNF-α, at different concentrations. Figure 2 shows that the compound **9** inhibited LPS-induced degradation and re-synthesis of IκBα protein, means dependently inhibited the phosphorylation of IκB (*α*-tubulin was used as control at same experiment conditions for both Western blot analysis experiments).

DISCUSSION

In summary, this study exhibited the separation and identification of 24 isolated compounds from the ethanolic extract of *E. prostrata* using chromatographic methods and spectroscopic data analysis. Subsequently, all the isolates **1**–**24** were evaluated for PTP1B and NO production inhibitory activities. In PTP1B assay, the active compounds **23** and **24** showed the strongest inhibition against PTP1B enzyme with IC_{50} values of 2.14 and 3.21 μM, respectively. Meanwhile, compounds **7** and **13**–**15** displayed significant inhibition on PTP1B enzymes. The enzyme kinetic analysis confirmed that compounds **7**, **13**, **14**, and **24** were mixed-type inhibitors and compounds **15** and **23** were competitive-type inhibitors. Interestingly, these active compounds isolated from *E. prostrata* were examined for their inhibitory activities on PTP1B for the first

time. Furthermore, molecular modeling studies were applied to explore how these compounds interact with the active sites or predict binding sites of PTP1B *via* evaluating the predicted binding energies. In this study, the ethanol extract of *E. prostrata* were confirmed more to be potent inhibitors both *in vitro* and *in silico*.

In NO assay, almost flavonoid and its derivatives (**1**–**4**, **7**, **8**, and **10**) exhibited strong inhibitory effects with IC_{50} values of 12.58, 15.67, 14.61, 12.16, 17.30, 12.77, 17.98 μM, respectively. Whereas, compounds **12**–**16** belonging to triterpenoids and tritepenoid glycosides, inhibited NO production in LPS-induced RAW264.7 with high IC_{50} values. The results suggested that the flavone and their glycosides are favor for NO inhibitory activity than triterpenoid and their glycosides. In addition, the flavones are more active than its derivative glycosides. Notably, 7-*O*-methylorobol-4′-*O*-*β*-D-glucopyranoside (**9**) potently inhibited NO production in LPS-stimulated RAW264.7 with IC_{50} value of 0.27 ± 0.01 μM. This compound may be benefit for development of inflammatory diseases. Western blot analyses further confirmed for inflammatory inhibition through IkB phosphorylation in RAW 264.7 Cells. The results demonstrated the protective effect of *E. prostrata* constituents on LPS-induced inflammatory response and the potential role of the NF-κB/IκB pathway in the anti-inflammatory activity of 7-*O*-methylorobol-4′-*O*-*β*-D-glucopyranoside.

Findings of the current study might approve for usage of this plant in herbal medicine for anti-diabetes, anti-obesity and anti-inflammatory activities. This study has much improvement for our understanding of biological activity from *E. prostrata* by supporting the active constituents.

Acknowledgments

This work was supported by the National Research Foundation of Korea (NRF) grant funded by the Korea government (NRF-2016R1D1A1B03931706).

Conflict of interest

The authors declare no conflict of ineterest.

Supplementary materials

The online version of this article contains supplementary materials.

REFERENCES

1) Koren S, Fantus IG. Inhibition of the protein tyrosine phosphatase PTP1B: potential therapy for obesity, insulin resistance and type-2 diabetes mellitus. *Best Practice & Research Clinical Endocrinology & Metabolism,* **21**, 621–640 (2007).

2) Klaman LD, Boss O, Peroni OD, Kim JK, Martino JL, Zabolotny JM, Moghal N, Lubkin M, Kim Y-B, Sharpe AH, Stricker-Krongrad A, Shulman GI, Neel BG, Kahn BB. Increased Energy Expenditure, Decreased Adiposity, and Tissue-Specific Insulin Sensitivity in Protein-Tyrosine Phosphatase 1B-Deficient Mice. *Mol. Cell. Biol.,* **20**, 5479–5489 (2000).

3) Zabolotny JM, Bence-Hanulec KK, Stricker-Krongrad A, Haj F, Wang Y, Minokoshi Y, Kim Y-B, Elmquist JK, Tartaglia LA, Kahn BB, Neel BG. PTP1B Regulates Leptin Signal Transduction *In Vivo*. *Develop. Cell,* **2**, 489–495 (2002).

4) Ying DL: The research progress in chemical constituents, pharmacological effects and clinic application of *Eclipta prostrata*. *Chin. Pharm.,* **26**, 2876–2877 (2008).

5) SP D, MP A: Study of Bhringaraja (*Eclipta alba*) therapy in jaundice in children. *J. Sci. Res. Pl. Med.,* **2**, 96–100 (1981).

6) Liu Q-M, Zhao H-Y, Zhong X-K, Jiang J-G. *Eclipta prostrata* L. phytochemicals: Isolation, structure elucidation, and their antitumor activity. *Food Chem.Toxicol.,* **50**, 4016–4022 (2012).

7) Tewtrakul S, Subhadhirasakul S, Tansakul P, Cheenpracha S, Karalai C. Antiinflammatory Constituents from *Eclipta prostrata* using RAW264.7 Macrophage Cells. *Phytother. Res.,* **25**, 1313–1316 (2011).

8) Lee J-S, Ahn J-H, Cho Y-J, Kim H-Y, Yang Y-I, Lee K-T, Jang D-S, Choi J-H. α-Terthienylmethanol, isolated from *Eclipta prostrata*, induces apoptosis by generating reactive oxygen species via NADPH oxidase in human endometrial cancer cells. *J. Ethnopharmacol.,* **169**, 426–434 (2015).

9) Ananthi J, Prakasam A, Pugalendi KV. Antihyperglycemic activity of *Eclipta alba* leaf on alloxan-induced diabetic rats. *Yale j. Biol. med.,* **76**, 97–102 (2003).

10) Kumari CS, Govindasamy S, Sukumar E. Lipid lowering activity of *Eclipta prostrata* in experimental hyperlipidemia. *J. Ethnopharmacol.,* **105**, 332–335 (2006).

11) Guo H, Callaway JB, Ting JPY. Inflammasomes: mechanism of action, role in disease, and therapeutics. *Nat. Med.,* **21**, 677–687 (2015).

12) Le DD, Nguyen DH, Zhao BT, Seong SH, Choi JS, Kim SK, Kim JA, Min BS, Woo MH. PTP1B inhibitors from *Selaginella tamariscina* (Beauv.) Spring and their kinetic properties and molecular docking simulation. *Bioorg. Chem.,* **72**, 273–281 (2017).

13) Lu X, Malumbres R, Shields B, Jiang X, Sarosiek KA, Natkunam Y, Tiganis T, Lossos IS. PTP1B is a negative regulator of interleukin 4-induced STAT6 signaling. *Blood,* **112**, 4098–4108 (2008).

14) Dat LD, Zhao BT, Hung ND, Lee JH, Min BS, Woo MH: Lignan derivatives from *Selaginella tamariscina* and their nitric oxide inhibitory effects in LPS-stimulated RAW 264.7 cells. *Bioorg. Med. Chem. Lett.,* **27**, 524–529 (2017).

15) Abdallah HM, Esmat A. Antioxidant and anti-inflammatory activities of the major phenolics from *Zygophyllum simplex* L. *J. Ethnopharmacol.,* **205**, 51–56 (2017).

16) Chen J, Teng J, Ma L, Tong H, Ren B, Wang L, Li W. Flavonoids isolated from the flowers of *Limonium bicolor* and their *in vitro* antitumor evaluation. *Pharmacog. Mag.,* **13**, 222–225 (2017).

17) Qiu D, Guo J, Yu H, Yan J, Yang S, Li X, Zhang Y, Sun J, Cong J, He S, Wei D, Qin J-C. Antioxidant phenolic compounds isolated from wild *Pyrus ussuriensis* Maxim. fruit peels and leaves. *Food Chem.,* **241**, 182–187 (2018).

18) Singh B, Sahu PM, Sharma RA. Flavonoids from *Heliotropium subulatum* exudate and their evaluation for antioxidant, antineoplastic and cytotoxic activities II. *Cytotechnology,* **69**, 103–115 (2017).

19) Awaad AS, Maitland DJ, Donia AERM, Alqasoumi SI, Soliman GA. Novel flavonoids with antioxidant activity from a Chenopodiaceous plant. *Pharm. Biol.,* **50**, 99–104 (2012).

20) Le J, Lu W, Xiong X, Wu Z, Chen W. Anti-Inflammatory Constituents from *Bidens frondosa*. *Molecules,* **20**, 18496–18510 (2015).

21) Han L-f, Zhao J, Zhang Y, Kojo A, Liu E-w, Wang T: Chemical Constituents from Dried Aerial Parts of Eclipta prostrata. *Chin. Herb. Med.,* **5**, 313–316 (2013).

22) El-Sohly HN, Joshi A, Li XC, Ross SA. Flavonoids from *Maclura tinctoria*. *Phytochemistry,* **52**, 141–145 (1999).

23) Yahara S, Ding N, Nohara T: Oleanane Glycosides from *Eclipta alba*. Chem. Pharm. Bull., **42**, 1336–1338 (1994).

24) Ye Y, Kinoshita K, Koyama K, Takahashi K, Kondo N, Yuasa H. New Triterpenes from *Machaerocereus eruca*. *J. Nat. Prod.,* **61**, 456–460 (1998).

25) Picher MT, Seoane E, Tortajada A. Flavones, sesquiterpene lactones and glycosides isolated from *Centaurea aspera* var. Stenophylla. *Phytochemistry,* **23**, 1995–1998 (1984).

26) Fernández MA, Sáenz MT, GarcÍA MD. Natural Products: Anti-inflammatory Activity in Rats and Mice of Phenolic Acids Isolated from *Scrophularia frutescens*. *J. Pharm. Pharmacol.,* **50**, 1183–1186 (1998).

27) Zhang Z, Liao L, Moore J, Wu T, Wang Z. Antioxidant phenolic compounds from walnut kernels (*Juglans regia* L.). *Food Chem.,* **113**, 160–165 (2009).

28) Nguyen DH, Le DD, Zhao BT, Ma ES, Min BS, Woo MH. Antioxidant Compounds Isolated from the Roots of *Phlomis umbrosa* Turcz. *Nat. Prod. Sci.,* **24**, 119–124 (2018).

29) Jin U-H, Lee J-Y, Kang S-K, Kim J-K, Park W-H, Kim J-G, Moon S-K, Kim C-H. A phenolic compound, 5-caffeoylquinic acid (chlorogenic acid), is a new type and strong matrix metalloproteinase-9 inhibitor: Isolation and identification from methanol extract of *Euonymus alatus*. *Life Sci.,* **77**, 2760–2769 (2005).

30) Choi HS, Cho J-Y, Jin MR, Lee YG, Kim S-J, Ham K-S, Moon J-H. Phenolics, acyl galactopyranosyl glycerol, and lignan amides from *Tetragonia tetragonioides* (Pall.) Kuntze. *Food Sci. Biotech.,* **25**, 1275–1281 (2016).

31) Cateni F, Falsone G, Zilic J, Bonivento P, Zacchigna M, Žigon D, Sosa S, Altinier G. Glyceroglycolipids from *Euphorbia nicaeensis All. with antiinflamatory activity*. *Arch. Org. Chem*., **5**, 54–56 (2004).

32) Zhao BT, Nguyen DH, Le DD, Choi JS, Min BS, Woo MH. Protein tyrosine phosphatase 1B inhibitors from natural sources. *Arch. Pharm. Res.,* **41**, 130–161 (2018).

Table 1. PTP1B and NO inhibitory activities of isolated compounds from *E. prostrata.*

Compounds	IC_{50} (μM)[a]		Enzyme kinetics	
	NO	PTP1B	K_i (μM)[b]	Inhibition type[c]
1	12.58 ± 0.18	82.40 ± 3.08	–	–
2	15.67 ± 0.01	81.77 ± 1.87	–	–
3	14.61 ± 0.32	>100	–	–
4	12.16 ± 0.13	45.50 ± 2.60	–	–
5	>50	>100	–	–
6	>50	>100	–	–
7	17.30 ± 0.13	14.11 ± 1.17	9.30	Mixed
8	12.77 ± 0.23	>100	–	–
9	0.27 ± 0.10	53.94 ± 1.45	–	–
10	17.98 ± 0.08	>100	–	–
11	85.27 ± 0.45	>100	–	–
12	>50	53.35 ± 3.96	–	–
13	>50	11.75 ± 0.20	9.97	Mixed
14	>50	15.23 ± 0.85	15.79	Mixed
15	>50	10.88 ± 0.97	11.65	Competitive
16	>50	>100	–	–
17	>50	>100	–	–
18	>50	>100	–	–
19	>50	>100	–	–
20	40.81 ± 0.14	>100	–	–
21	>50	48.70 ± 5.50	–	–
22	>50	59.87 ± 5.48	–	–
23	>50	2.14 ± 0.09	2.01	Competitive
24	>50	3.21 ± 0.13	3.39	Mixed
Ursolic acid[d]	–	12.00 ± 0.71	–	–

[a]The IC_{50} values (μM) were calculated from a log dose inhibition curve and are expressed as mean ± SD of triplicate experiments. [b]PTP1B inhibition constants (μM) of tested compounds determined using secondary plot of the *slopes* and *y-intercept* of each linear regression of Lineweaver-Burk plot [c]PTP1B inhibition types of tested compounds determined using Lineweaver–Burk plots. [d]Positive controls. (–) Not tested.

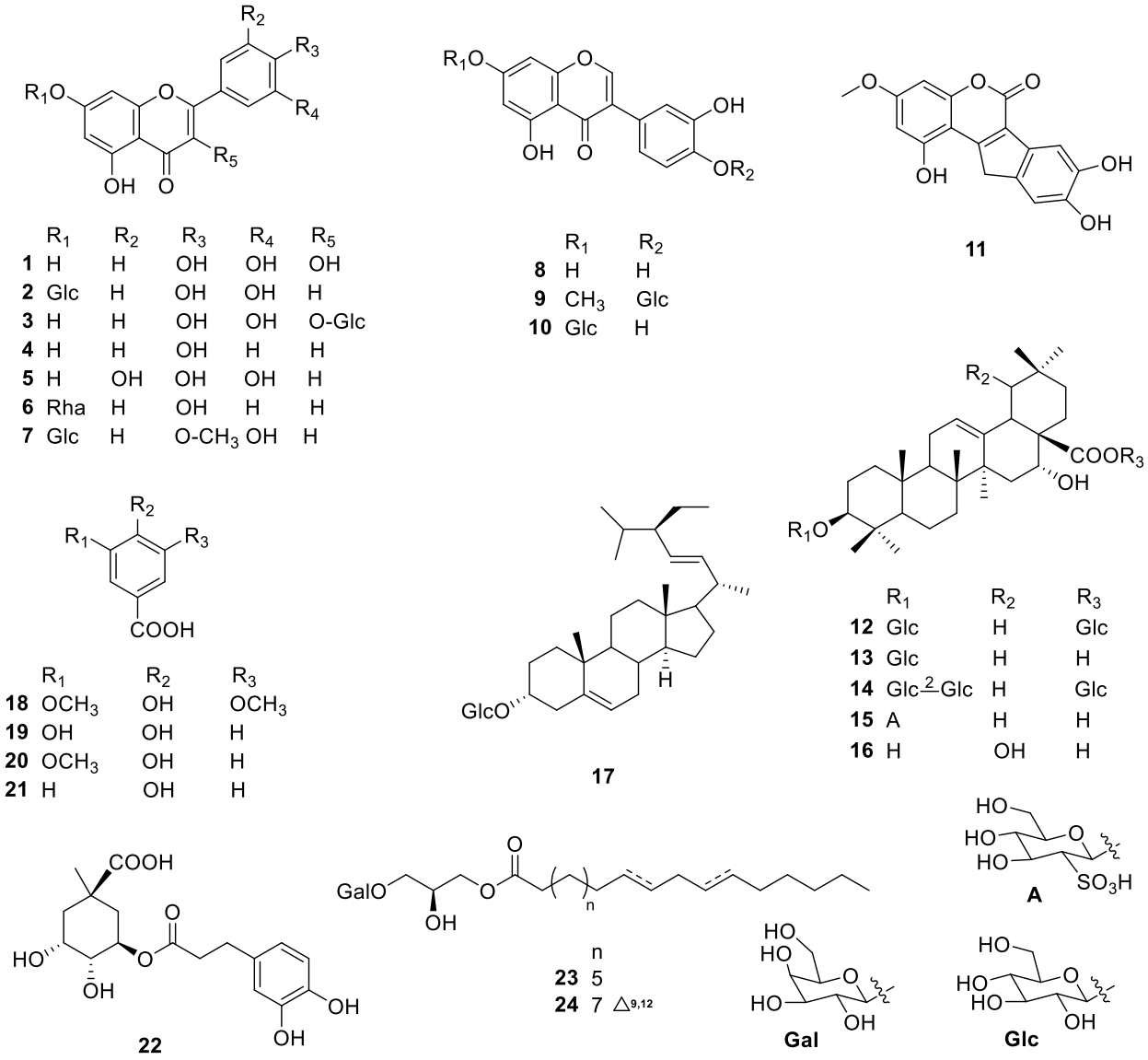

Figure 1. Structures of isolated compounds from *E. prostrata*.

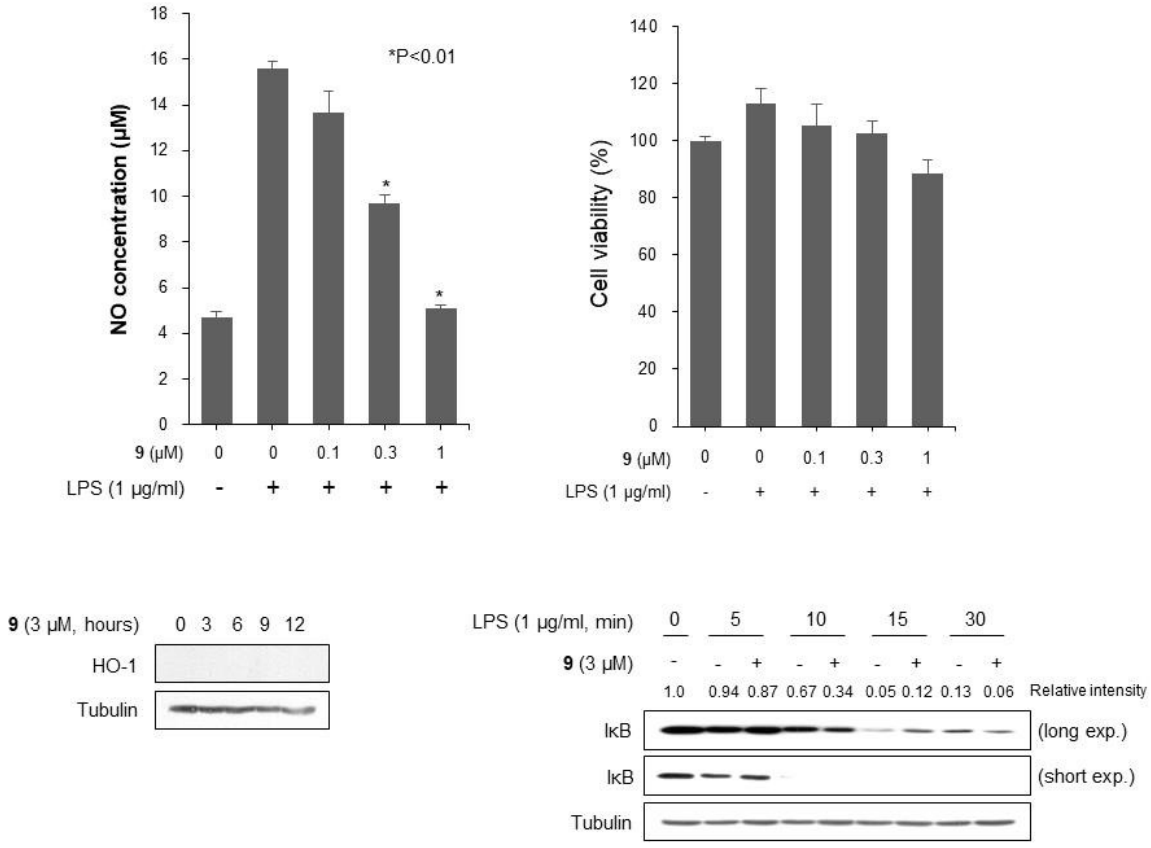

Figure 2. Inhibitory effect of LPS-induced IκB and HO-1 expression in RAW264.7 cells by compound **9**.